

Cite this: *Soft Matter*, 2011, **7**, 5246

www.rsc.org/softmatter

PAPER

# A high-performance magnetorheological material: preparation, characterization and magnetic-mechanic coupling properties†

Yangguang Xu, Xinglong Gong,\* Shouhu Xuan,\* Wei Zhang and Yanceng Fan

Received 20th February 2011, Accepted 21st March 2011

DOI: 10.1039/c1sm05301a

A novel high-performance magnetorheological material, named as magnetorheological plastomer (MRP), was developed by dispersing iron particles into a plastic polyurethane (PU) matrix. The dynamic properties (including storage modulus and loss factor) of the MRP material were systematically tested and the influences of the iron particle content and magnetic field were analyzed. It is found that the anisotropic MRP product with 80% iron particle weight fraction (A-MRP-80), shows a high dynamic property: the maximum magneto-induced storage modulus is 6.54 MPa; the relative MR effect reaches as high as 532%; the loss factor can be reduced to 0.03 by adjusting magnetic field. This kind of MRP shows a much higher magnetorheological performance than the previously reported magnetorheological elastomer (MRE). The mechanism for its high MR performance was proposed and the influence of the iron particle distribution and temperature on the dynamic properties were discussed.

## 1. Introduction

Magnetorheological (MR) materials are a type of smart material which has attracted increasing attention since their unique rheological properties can be changed continuously, rapidly and reversibly, by applying a magnetic field. Due to their wide applications in architecture, vibration control, and automotive industry, *etc.*, many works have been reported on the synthesis of MR material.<sup>1</sup> Normally, MR materials are prepared by dispersing micrometre sized soft magnetic particles into a carrier matrix. According to the state of matrix, MR materials can be classified into MR fluids, MR gels, MR foams, and MR elastomers.<sup>1–4</sup> The firstly developed MR material was MR fluids (MRF), which are liquid suspensions of ferromagnetic particles whose yield stress and viscosity can change by two or three orders of magnitude under a magnetic field. The mechanism of MRF is extensively studied<sup>5–7</sup> and its applications in damper,<sup>8</sup> brake,<sup>9</sup> vibration control,<sup>10</sup> and isolator,<sup>11</sup> *etc.* have been widely developed. However, the problems such as particle sediment, stability and leakage in application devices preclude its further development. To solve these problems, polymer matrices with high viscosity are employed to carry ferromagnetic particles and the as-named MR gels (MRG) and MR elastomers (MRE) are developed.<sup>12–16</sup>

For MRE, the storage modulus and loss factor can be controlled by tuning the externally applied magnetic field, which enables their use in suspension systems, engine mounts, bushing, and tunable vibration absorber,<sup>17–21</sup> *etc.* MRE with high magneto-induced modulus and MR effect can provide new opportunities for improving its performance in practical application. The mechanic properties of the MRE are dependent on many aspects. Bellan *et al.* found that the MR effect of MRE increased with the increasing of iron particle content and the pre-configuration process.<sup>22</sup> Besides the weight ratio, the size of the magnetic particle also influences the MR effect and the MRE with large iron particles show a high MR effect.<sup>23</sup> Chen *et al.* experimentally investigated the influences of matrix type, external magnetic flux density, and temperature in the stage of forming pre-configuration, content of plasticizers and iron particles on the performance of the natural rubber based MRE. With these guidelines, a natural rubber based MRE with a 133% relative MR effect and 3.6 MPa of the magneto-induced storage modulus was prepared.<sup>24</sup> However, the relative MR effect of the previous reported MR materials is relatively small, which confines their practical applications.

The silicon rubber based MRE can reach a high relative MR effect, but its magneto-induced storage modulus is not large enough. Gong *et al.* reported a new method to prepare silicone rubber based MRE and its MR effect can reach 878%. However, the magneto-induced storage modulus is small (3 MPa) and the high MR effect is mainly due to its low initial storage modulus (0.34 MPa).<sup>25</sup> Recently, Chertovich *et al.* reported a new kind of composite elastomers with a 41900% relative MR effect. Unfortunately, their storage modulus can only increase from 0.001 MPa to 0.42 MPa when the external magnetic field

CAS Key Laboratory of Mechanical Behavior and Design of Materials, Department of Modern Mechanics, University of Science and Technology of China (USTC), Hefei, Anhui, 230027, China. E-mail: gongxl@ustc.edu.cn; Tel: +86 551 3600419; Fax: +86 551 3600419; xuansh@ustc.edu.cn; +86 551 3606382; +86 551 3600419

† Electronic supplementary information (ESI) available: Supplementary information. See DOI: 10.1039/c1sm05301a

increases from zero to 300 mT.<sup>26</sup> An ideal MR material should possess both a high relative MR effect and a high magneto-induced storage modulus. Therefore, more work should be focused on developing high performance MR materials not only for the fundamental interest but also for their practical applications.

The matrix has a big influence on the dynamic properties of MRE, therefore a suitable matrix should be employed to synthesize MRE with desirable magneto-induced storage modulus and relative MR effect. Among the various polymer matrixes, polyurethane (PU) materials are of great interest as they have better degradation stability than natural rubber and superior mechanical performance than silicon rubber. Interestingly, it is found that the initial storage modulus and loss factor of the PU can be changed by adjusting the ratio of raw materials. Very recently, our group prepared a polyurethane (PU) based MRE whose magneto-induced storage modulus reached 4.9 MPa while relative MR effect was 121%.<sup>27</sup> Based on that work, a high performance MRE can be successfully synthesized. The MR materials using PU as the matrix, with tunable dynamic properties, can be obtained by varying the PU characteristics. To this end, a PU based MR material with high magneto-induced storage modulus and high relative MR effect is very desirable.<sup>15,27–30</sup>

Here, we reported a new MR material with high performance dynamic properties. The matrix of this MR material is a low molecular weight polyurethane, a elastomer which was synthesized by using toluene diisocyanate (TDI) and polypropylene glycol (PPG-1000). Different from the PU based MRE, the as-prepared MR materials show plastic properties at room temperature, which can be defined as MR elastomer (MRP). Both the isotropic MRP (I-MRP) and the anisotropic MRP (A-MRP) were successfully prepared. The influence of the magnetic field, iron particle content, iron particle distribution and temperature on dynamic properties of this MR material were investigated. In addition, the microstructures of this material with different iron particle content and pretreatment process were observed and the mechanism for the high MR performance was discussed. To the best of our knowledge, this is the first report on MRP and this kind of MR material shows higher MR performance than the previously reported MR elastomers (MRE).

## 2. Experimental

### 2.1 Raw materials

Toluene diisocyanate (TDI; 2,4- $\approx$ 80%, 2,6- $\approx$ 20%, Tokyo Chemical Industry Co., Ltd, Japan) and polypropylene glycol (PPG-1000,  $M_n = 1000$ , The Third Petrochemical Factory, Tianjin Petrochemical Inc, China) were selected as the main reactants. The polypropylene glycol (PPG-1000,  $M_n = 1000$ ) was distilled at 90 °C $\sim$ 100 °C in a vacuum for about 1 h before used. 1,4-Butanediol (BDO, Sinopharm Chemical Reagent Co., Ltd, China) was used as a chain extender and stannous octoate (Sinopharm Chemical Reagent Co., Ltd, China) was used as the catalyst. Acetone (Sinopharm Chemical Reagent Co., Ltd, China) was selected as solvent when needed. Carbonyl iron particles (type CN) (provided by BASF in Germany with the size

distribution:  $d_{10} = 3.5 \mu\text{m}$ ,  $d_{50} = 6 \mu\text{m}$ ,  $d_{90} = 21 \mu\text{m}$ ) were used as the magnetic particles dispersed in the matrix.

The ratio of TDI and PPG was calculated by the formula below:

$$\frac{n_{\text{NCO}}}{n_{\text{OH}}} = \frac{m_{\text{TDI}}/174.15\text{g}\cdot\text{mol}^{-1}}{m_{\text{PPG}}/1000\text{g}\cdot\text{mol}^{-1}}$$

Where  $n_{\text{NCO}}$  is the mol of –NCO group,  $n_{\text{OH}}$  is the mol of –OH group,  $m_{\text{TDI}}$  is the weight of TDI and  $m_{\text{PPG}}$  is the weight of PPG.

The molar ratio of  $n_{\text{NCO}}$  and  $n_{\text{OH}}$  was set as 3 : 1 for better dynamic properties according to the research of Wei.<sup>27</sup> The weight of BDO added at the phase of chain extension was calculated by the following formula.  $m_{\text{BDO}}$  indicates the weight of BDO.

$$\begin{aligned} \frac{n_{\text{NCO}}}{n_{\text{OH}}} &= \frac{(m_{\text{TDI}}/174.15\text{g}\cdot\text{mol}^{-1}) \times 2}{(m_{\text{PPG}}/1000\text{g}\cdot\text{mol}^{-1}) \times 2 + (m_{\text{BDO}}/90.12\text{g}\cdot\text{mol}^{-1}) \times 2} \\ &= 1.1 \end{aligned}$$

### 2.2 Sample preparation

There are three steps in the synthesis of the matrix. Firstly, TDI and PPG were added to a 250 mL three-necked round bottom flask with a stirrer agitating the reactants all the time, the temperature of reaction system is 75 °C. 2 h later, BDO was added into reactor and at the same time the temperature was reduced to 65 °C. This phase lasted about 1 h. Finally, stannous octoate (0.15 g) was added into flask at 60 °C, when the viscosity of reactant increased obviously, the reaction was stopped. During the reaction, moderate acetone was added to avoid gelation.

The iron particles were added into the matrix by vigorously stirring for a long enough time until the matrix and iron particles were well mixed before the matrix cooled down. Then the product was placed at room temperature for 72 h. Four kinds of products with 40 wt%, 60 wt%, 70 wt%, and 80 wt% of iron particle content were prepared. The four kinds of products were named as MRP-40, MRP-60, MRP-70, and MRP-80, respectively. In addition, the matrix without any iron particles for comparison purposes was also prepared.

### 2.3 Properties characterization

A Bruker FTIR (EQUINOX55) spectrometer was used to collect the Fourier transform infrared (FTIR) spectra of the matrix and MRP-60 in the range 4000–500  $\text{cm}^{-1}$  at room temperature.

The microstructures of the MRP products with different pretreatment processes were observed by a digital microscope (VHX-200, Keyence Co., Japan). The I-MRP products with different iron particle content were evenly smeared on the surface of slide glasses. The A-MRP products were prepared by applying an external magnetic field (800 mT) for 10 min (this process is named as pre-configuration) before the observation. In addition, the microstructures of A-MRP-70 and I-MRP-70 were also characterized by environmental scanning electron microscopy (SEM, Philips of Holland, model XT30 ESEM-MP) with an accelerating voltage of 20 kV. The two kinds of MRP-70 were

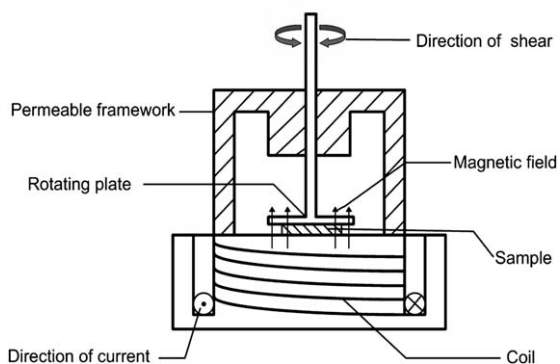


**Fig. 1** Principle of testing part for Physica MCR 301.

placed into liquid nitrogen until they were frozen into pieces and suitable cross sections were chosen for observation.

A commercial rheometer (Physica MCR 301, Anton Paar Co., Austria) was used to test the dynamic properties of the MRP products. Fig. 1 shows the schematic of the testing part. The sample is placed between two parallel plates and a shear strain loading is applied on the sample through the rotating plate, which is made of non-permeable material. Two arrows as shown in Fig. 1 indicate the direction of the dynamic shear. The rotating plate can also transmit other signals (such as stress, displacement, and temperature, *etc.*) by the sensors connecting to it. The magnetic field is generated by an inbuilt coil and the value of the magnetic field is controlled by the current in the coil. Magnetic field lines pass through a permeable framework and sample to form a closed magnetic circuit.

The MRP sample was prepared just like a disc whose diameter was 20 mm and thickness was 1 mm. Shear oscillation mode was taken to test the dynamic properties. The amplitude of shear strain was set as 0.2% (this value can make sure the testing data fall in the linear viscoelastic regime according to a series of previously stress-strain curves tested for MRP materials), the oscillation frequency was 5 Hz, and the range of magnetic flux density was 0–860 mT by adjusting the coil current from 0 A to 3.6 A. All the tests were carried out at room temperature unless otherwise stated.

### 3. Results and discussion

#### 3.1 Synthesis and microstructures of the MRP materials

In our work, as soon as the PU matrix was synthesized, iron particles were added and well dispersed in the matrix. After aging for 72 h, an iron/PU composite, which can be named as MRP, was obtained. The FTIR spectra were used to characterize the as-prepared products (Fig. 2). Fig. 2a shows the typical FTIR spectrum of the pure matrix in the range 4000–500  $\text{cm}^{-1}$ . The peaks located at 3290 and 1534  $\text{cm}^{-1}$  are attributed to the  $-\text{NH}_2$  stretching band and deformation vibration band, whilst the band at 1728  $\text{cm}^{-1}$  is related to the carbonyl  $\text{C}=\text{O}$  stretching. These three bands are the characteristic bands of PU, which proves that PU has been successfully synthesized. The peak at 1106  $\text{cm}^{-1}$  is ascribed to an ether  $\text{C}-\text{O}-\text{C}$  group, indicating that TDI and PPG have taken part in the reaction. The  $-\text{NCO}$  band appears at 1450  $\text{cm}^{-1}$  which means that there is a portion of TDI in the

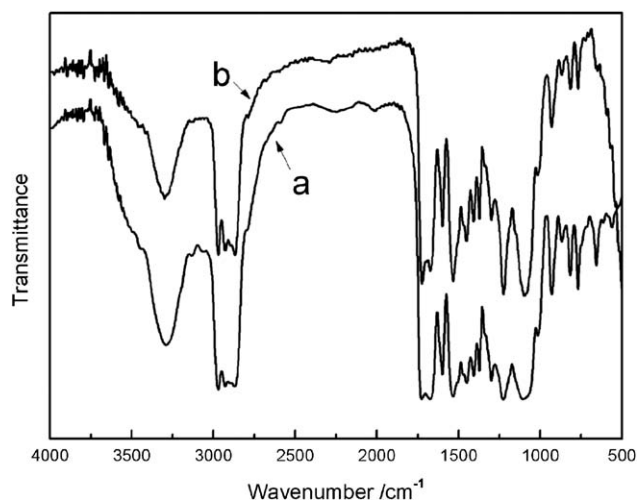


**Fig. 2** FTIR spectra of PU matrix and MRP-60 in the range of 4000–500  $\text{cm}^{-1}$ : (a) the matrix; (b) the MRP-60.

matrix. In addition, the symmetric stretching of methylene  $\text{CH}_2$  and methyl  $\text{CH}_3$  appears at 2870  $\text{cm}^{-1}$  while the asymmetric stretching of methyl  $\text{CH}_3$  is observed at 2971  $\text{cm}^{-1}$ . The above analysis indicates that the PU matrix is a mixture of polyurethane and TDI. Fig. 2b shows the FTIR spectrum of MRP-60. In comparison with Fig. 2a and 2b, it is very clear that the MRP material is composed of a PU matrix and iron particles.

Different from our previously reported PU based MRE (PPG-2000 was used as the raw material), the as-prepared MRP displays plastic properties at room temperature. Fig. 3 shows the photograph of the MRP material, which indicates that the MRP material is very similar to the plasticene and the shapes of the product can be changed to various forms and the shapes can be kept if no external force is applied to it. Obviously, particle sediment phenomenon cannot be found in this new MRP material. In addition, the product can be divided into pieces and these separated blocks can be integrated to one block, which indicates that it has a self-curable property at room temperature.

The reason for such phenomenon may be attributed to the following three aspects: Firstly, the PPG-1000 was selected as the

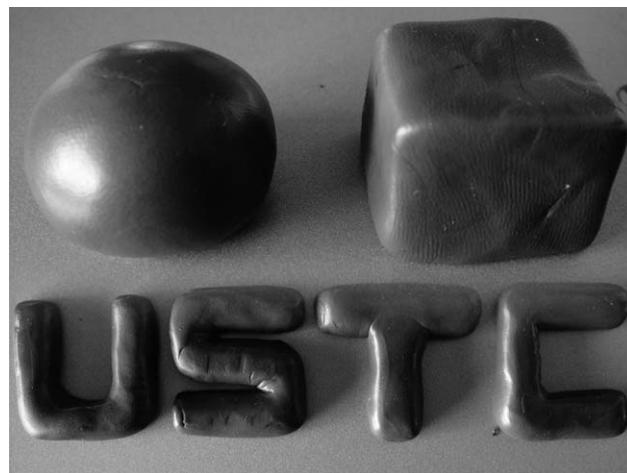


**Fig. 3** Photograph of MRP-80 with different forms.

reactant. In comparison to commonly used PPG-2000, PPG-1000 has a lower molecular weight and a shorter chain segment, therefore the molecular weight of the PU matrix is relatively low which enables the as-prepared MRP material to show plastic characteristics. Secondly, it is reported that the ratio of rigid segments (provided by TDI) and soft segments (provided by PPG) determines the viscosity of matrix.<sup>27,31</sup> In our product, the ratio of  $n_{\text{NCO}}$  and  $n_{\text{OH}}$  was set as 3 : 1, which indicates that the as-prepared polymer is a soft matrix. lastly, according to the FTIR analytical results, there is a portion of TDI still in the matrix which does not form the construction of physical cross-linking. This part of TDI exists in the matrix independently in the form of macromolecule which will also soften the matrix. The conventional MRF and MRG are viscous liquids and the as-prepared MRP material shows a solid state. However, the MRP also cannot be classified into MRE due to its special plastic physical properties. Therefore, this new PU based MR material was defined as MR palstomer (MRP) and it is an intermediate state between MRG and MRE.

In this work, two kinds of MRP materials with different iron particle distribution can be achieved. For the freshly prepared MRP materials, all the iron particles are well dispersed in the matrix in an isotropic state. Therefore, this kind of MRP is named as isotropic MRP (I-MRP). In the second case, the isotropic MRP was treated under a pre-configuration process. Here, the pre-configuration was conducted by applying an 800 mT magnetic field to the product for 10 min. After the pre-configuration, the MRP materials are anisotropic and the iron particles are assembled to form chain like structures aligned parallel to the magnetic field direction. This material is defined as anisotropic MRP (A-MRP). Our experiment found that 10 min pre-configuration is long enough to re-assemble the iron particles and a longer pre-configuration time shows little influence on dynamic properties (Fig. S2, ESI†). The A-MRP material shows a stable structure and mechanical properties in our study.

Optical microscopy and environmental scanning electron microscopy were used to investigate the microstructures of these two kinds of MRP products. The white bright spots in Fig. 4a and

4b stand for the position of the iron particles and the dark background is the matrix. A homogeneous distribution of the particles can be observed in Fig. 4a and 4c, which proves the freshly prepared MRP materials are isotropic. After pre-configuration, the iron particles tend to aggregated into strings as shown in Fig. 4b and 4d. Fig. 4b is for the A-MRP-60, it is found that all the iron particles are assembled to form chain like structures aligned parallel to the magnetic field direction as expected. However, further increasing the proportion of the iron particles (as shown in Fig. S1, ESI† where Fig. S1e–h is for A-MRP-40, A-MRP-60, A-MRP-70, and A-MRP-80, respectively), it becomes more and more difficult to distinguish particle chains because they are close to each other. Fig. 4d also indicates that the pre-configured MRP is anisotropic.

The magnetic field has an important influence on the distribution of iron particles in the MRP products. As soon as a magnetic field is applied to the MRP material, the dipole magnetic force drives the iron particles to get close to each other and form particle chains, aligned with the magnetic field direction, which is similar with the pre-configuration of MRE. However, the iron particle chains are fixed in the matrix of MRE after preparation and hardly move, even under a strong magnetic field. The iron particles in MRP are movable and can transform their locations to form new chains aligned with the direction of magnetic field (but if the direction of the magnetic field is parallel with the iron particles chain, the iron particles in MRP can hardly be moved too). This self-assembling property, which can be controlled by magnetic field, will make the MRP more intelligent in practical applications.

### 3.2 Dynamic properties for the anisotropic MRP materials

The relationship between shear storage moduli ( $G'$ ) of the A-MRP with different iron particle content and magnetic flux density is shown in Fig. 5. Taking A-MRP-80 for example,  $G'$  shows an increasing tendency with the increasing of the magnetic field at first and then tends to level off. It can be seen from Fig. 5 that the iron particle content has a great influence on  $G'$ , the

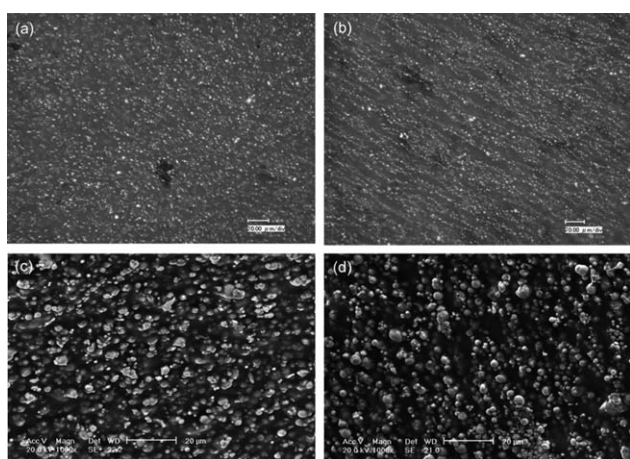


**Fig. 4** Microstructures of MRP with different iron particle distribution: (a) optical microscopy image of I-MRP-60; (b) optical microscopy image of A-MRP-60; (c) SEM image of I-MRP-70; (d) SEM image of A-MRP-70. The scale bar on the images corresponds to 20 microns.

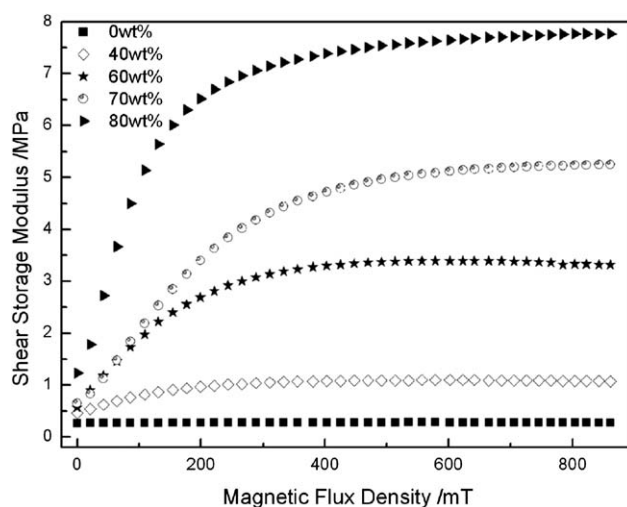


**Fig. 5** Storage moduli of A-MRP with different iron particle content under different magnetic flux density.

MRP with higher iron particle content often have a higher  $G'$ , which is similar to MRE.<sup>24</sup> For example, the maximum  $G'$  of the A-MRP-80 is 7.77 MPa, while the maximum  $G'$  of the A-MRP-70 is 5.25 MPa. It can be seen from Fig. 5 that  $G'$  of the matrix almost remains at a constant value, thus the magneto-induced modulus ( $\Delta G'$ ) is mainly caused by the magnetic particle interactions.

The magnetic properties of A-MRP with different iron particle content were investigated by MPMS VSM (SQUID, Quantum Design Co., America). Fig. 6 shows the magnetic hysteresis loops of the as-prepared A-MRP with different iron particle content, which indicate that every product exhibits a soft magnetic characteristic. Their magnetization ( $M$ ) increase with increasing magnetic flux density at first and then tend to a constant value. The dependence of  $M$  on the magnetic field in the first quadrant of Fig. 6 is similar to the dependence of  $\Delta G'$  on magnetic field shown in Fig. 5. The similarity is not accidental and a magnetic dipole model<sup>32</sup> can be used to explain the relationship between  $M$  and  $\Delta G'$ . The iron particles in the A-MRP material are magnetized under an external magnetic field. In the direction of magnetic field, the magnetic force is an increasing function of magnetic dipole moment ( $m$ ) and  $m$  is proportional to  $M$ . In particular, the magnetic force is linear function of  $m$  under uniform magnetic field.<sup>33</sup> As a result, the magnetic force is proportional to  $M$  too. The  $M$  for magnetic particles increases with the increasing of the magnetic field at first and then tends to level off. In addition, under a certain magnetic field, the A-MRP material with higher iron particle content often has a larger  $M$ . The magnetic force is proportional to  $\Delta G'$ , that is to say,  $\Delta G'$  is a linear function of  $M$ . Therefore, a similar law is reflected in  $\Delta G'$  which is shown in Fig. 5.

The initial storage modulus ( $G'_0$ , the storage modulus without magnetic field) increases with the increasing of the iron particle content (Fig. 5), which indicates that the existence of iron particles will enlarge the hardness of the A-MRP product. Table 1 shows  $G'_0$  and  $\Delta G'$  values of the A-MRP products with different iron particle content. The data shown in Table 1 agrees well with the analytical results. Additionally, it is found that the relative increment of  $\Delta G'$  is not always larger than that of  $G'_0$ , in

**Table 1** The initial storage moduli, magneto-induced moduli and relative MR effect of the A-MRP with different iron particle content

Iron particle content	Initial storage modulus $G'_0$ /MPa	Magneto-induced modulus $\Delta G'$ /MPa	Relative MR effect $\Delta G'/G'_0$
40 wt%	0.465	0.63	136%
60 wt%	0.57	2.68	470%
70 wt%	0.65	4.6	708%
80 wt%	1.23	6.54	532%

consequence, the relative MR effect does not increase with the increasing of iron particle content. For example, if the iron particle content increases from 70 wt% to 80 wt%, the relative MR effect of the A-MRP product is not increase but decreases from 708% to 532%.

An ideal MR material should possess both a high relative MR effect and a high magneto-induced storage modulus. The MR effect and magneto-induced storage modulus of the as-prepared A-MRP-80 can reach to as high as 532% and 6.54 MPa, which are better than that for MRE. In previous reports, although the relative MR effect of the silicon rubber based MRE can reach to 775%, the high relative MR effect is mainly due to its low initial storage modulus (about 0.32 MPa) and its magneto-induced storage modulus (about 2.48 MPa) is very small.<sup>34</sup> For the natural rubber based MRE,  $\Delta G'$  is 3.6 MPa and relative MR effect is 133%.<sup>24</sup> In this work, the PU based A-MRP-80 shows higher values (6.54 MPa and 532%). In comparison with our previously synthesized PU based MRE, the as-prepared A-MRP-80 also exhibits a higher  $\Delta G'$  and relative MR effect.<sup>27</sup> Moreover, for most of the reported MRE,  $G'$  is not sensitive to magnetic field under a low magnetic field and it will change acutely only when the magnetic field reaches above a certain value (about 200 mT). Different from MRE, the present A-MRP is very sensitive to the magnetic field. The  $G'$  of the A-MRP increases sharply as soon as the magnetic field is increased from zero. When the magnetic field increases to 300 mT,  $G'$  is almost saturated. This result indicates that the MRP is a high magneto-sensitive material.

The matrix of the MRP material is a plastomer, which is softer than the one for MRE based on nature rubber and polyurethane, thus  $G'_0$  of the A-MRP is smaller than that of MRE. For the I-MRP, the iron particles distributed homogeneously in the matrix (as shown in Fig. 7a) can move easily within the matrix under a magnetic field. Increasing the magnetic field, the iron particles will eventually form chains aligned with the direction of magnetic field, which can be observed in Fig. 4. These particle chains run through the whole material (as shown in Fig. 7c) and this phenomenon is different from the finite length particle chains formed in MRE.<sup>35</sup> Under a certain shear strain, longer particles chains and higher magnetic field often lead to larger magnetic interactions between the iron particles, which will lead to a larger  $G'$ . In this case, due to the high  $\Delta G'$ , the A-MRP material shows a high MR effect. Furthermore, the matrix of the A-MRP is too soft to sustain shear loading, thus the magnetic interactions between iron particles is the main factor resisting the shear strain. The magnetic interactions are highly dependent on the magnetic field, thus  $G'$  is high-sensitive to the magnetic field. However,

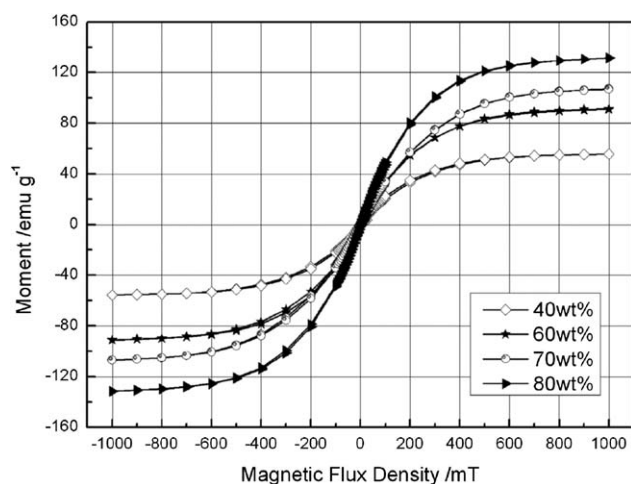


**Fig. 6** Magnetic properties of A-MRP with different iron particle content under different magnetic flux density.

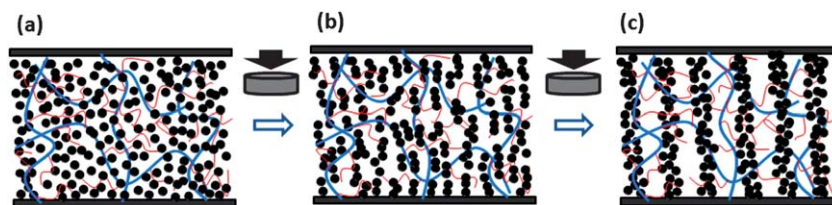


**Fig. 7** Schematic diagram of the pre-configuration process of MRP under an external magnetic field: (a) the isotropic MRP; (b) the low anisotropic MRP; (c) the anisotropic MRP. The two black solid arrows indicate the direction of magnetic field. Blue thick curves indicate the hard segments in PU and the red thin ones indicate the soft segments.

when a small magnetic field is applied to the MRE, the shear loading is mainly applied to the matrix. The  $G'$  of the matrix remains almost constant, therefore, the  $G'$  of MRE increases slowly at first. Further increasing of magnetic field, the contribution of the magnetic interactions between the iron particles to  $G'$  increases and  $G'$  begins to increase notably. Therefore, the  $G'$  of MRE is not sensitive to a low magnetic field.

The magnetic field dependency of the loss factors ( $\tan\delta = G''/G'$ , where  $G'$  indicates the storage modulus which represents the ability of storing the energy of deformation.  $G''$  indicates the loss modulus which represents the ability of dissipating the energy of deformation) is shown in Fig. 8. It is found that  $\tan\delta$  of the A-MRP with high iron particle content shows a sharper decrease with magnetic field compared with the one with low iron particle content. At low magnetic field,  $\tan\delta$  decreases sharply with increasing magnetic field, and then tends to level off with further increasing of magnetic field. This phenomenon is a unique damping property for the MRP material, which has not been found from other MR materials. As can be seen from Fig. 8,  $\tan\delta$  of matrix is almost independent on the externally applied magnetic field. Therefore, the decreasing of  $\tan\delta$  of the A-MRP material may be attributed to the magnetic interactions between the iron particles. It was reported that the  $\tan\delta$  of MRE only changes a little under an external magnetic field and its value increases with the increasing of the iron particles content.<sup>24</sup> However, in this work,  $\tan\delta$  shows a decreasing trend with increasing of magnetic field and its value can be changed from

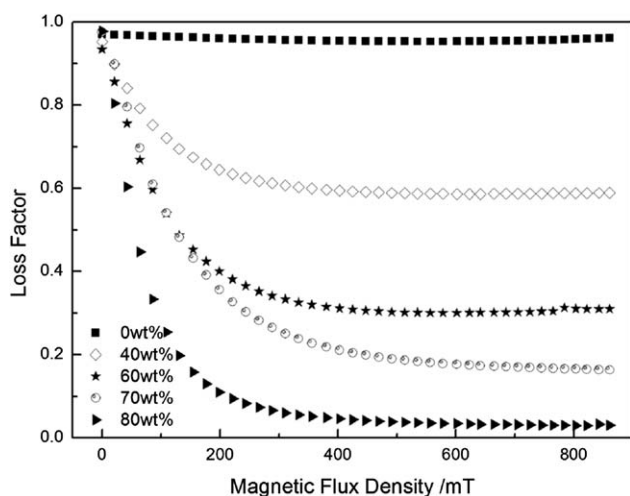


**Fig. 8** Loss factors of A-MRP with different iron particle content under different magnetic flux density.

0.97 to 0.03 when the magnetic field increases from 0 mT to 300 mT, taking A-MRP-80 for example. For some practical applications, it hopes that  $\tan\delta$  should be as low as possible and the tuning range should be easily controlled by magnetic field. In this case, the damping property of A-MRP is more ideal than that of MRE.

The damping of this kind of composite material mainly comes from the damping of the composites (matrix and iron particles) and the energy dissipation which is caused by the interfacial slipping.<sup>36,37</sup> The damping of particles can be ignored compared with that of the matrix, and the damping of matrix mainly comes from the movement of the soft segments in polyurethane.<sup>27</sup> After pre-configuration, the particles have been arranged in suitable positions which can hardly be moved when a magnetic field is applied to the A-MRP parallel to the particle chains. Therefore the energy dissipation caused by interfacial slipping can be ignored too. With the increasing of magnetic field, the magnetic interactions between iron particles increase, which will prevent the movement of the soft segments in the matrix (as shown in Fig. 7c). The damping from the matrix will decrease because the movement of the soft segments is restricted. When the magnetic field increase to a certain value (300 mT), the magnetic interactions are almost saturated and the restriction effect to the soft segments achieves a maximum. As a result, the damping tends to a plateau value. Under a similar magnetic field, the magnetic interactions between the iron particles increases with the increasing of the iron particle number. The large magnetic interactions lead to a large restriction effect to soft segments, which further leads to a low energy dissipation. Then, a small  $\tan\delta$  is achieved.

### 3.3 Influence of iron particle distribution on the dynamic properties

In order to fully understand the MRP material, the influence of the iron particle distribution on the dynamic properties is also systematically investigated. As shown in Fig. 4, the arrangement of the iron particles changes a lot when an external magnetic field is preliminarily applied. Here, MRP-80 was employed as an example. A piece of freshly prepared MRP-80 was divided into several identical parts, one part was placed in a magnetic field (800 mT) for 10 min (the synthesis of A-MRP) before testing and the other parts were used directly for testing.

The magnetic field dependence of  $G'$  for the I-MRP-80 and A-MRP-80 is shown in Fig. 9. It is found that the  $G'$  of I-MRP-80 is lower than that of A-MRP-80 under the same magnetic field. Interestingly, the magneto-induced modulus ( $\Delta G'$ ) of I-MRP-80

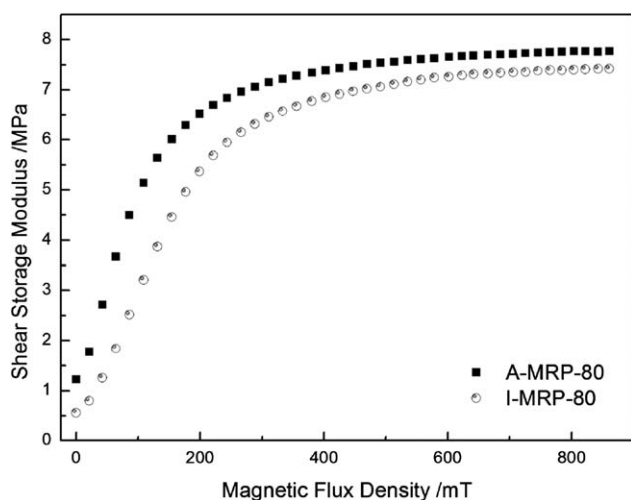


**Fig. 9** Storage moduli of MRP-80 with different pretreatment process under different magnetic flux density.

is higher than that of A-MRP-80, which leads to a higher relative MR effect for I-MRP-80 than A-MRP-80 (as shown in Table 2).

In order to clarify how the iron particle distribution affects the dynamic properties of the MRP, a comparison testing was carried out. Fig. 10a (part of Fig. 9) shows the dependence of the  $G'$  of I-MRP-80 on a magnetic field ranges 350–800 mT, which indicates that the  $G'$  increases continuously with increasing magnetic field. In a comparison experiment, as soon as the testing magnetic field was increased to 450 mT, the testing was stopped and the product was then treated under a 450 mT magnetic field. 10 min later, the testing continued. Interestingly,  $G'$  shows a sharp increment (Fig. 10b) in comparison to the non-treated one (Fig. 10a). If the treating field is increased to 800 mT (10 min), the increment increases to an even higher one (Fig. 10c), which clearly indicates that the pre-configuration has a crucial effect on the dynamic properties of the MRP. Notably, the  $G'$  of the MRP treated under an 800 mT magnetic field (10 min) during the testing process (at the 450 mT testing magnetic field point) shows similar behavior to the  $G'$  of the fully pre-configured MRP (Fig. 10d and part of Fig. 9) under the testing field 450–800 mT. In our case, the iron particles in the I-MRP (as shown in Fig. 7a) will rearrange under a magnetic field and tend to form particle chains aligned with the magnetic field. If the magnetic flux density is low and the time of the pre-configuration is not long enough, the particle chains are short (as shown in Fig. 7b). In this case, the product can be defined as low anisotropic MRP. The magnetic interactions in the low anisotropic MRP are smaller than that of the full pre-configured MRP (as shown in Fig. 7c). Thus, the low anisotropic MRP often gets a larger  $G_0'$

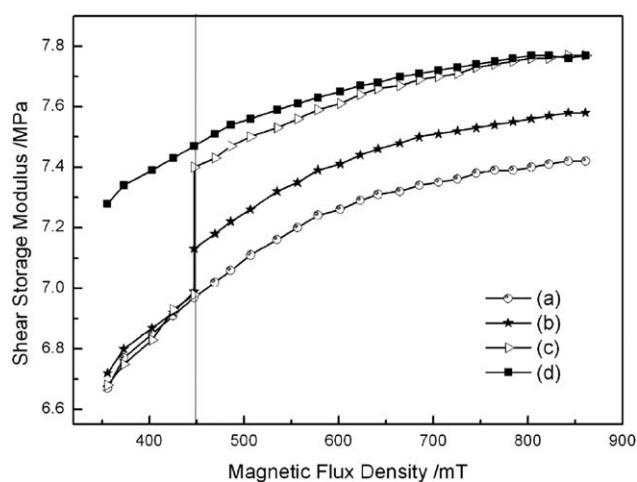


**Fig. 10** Storage moduli of MRP-80 with different processing method under different magnetic flux density: (a) without pre-configuration and other processing method; (b) a 450 mT magnetic field was applied to I-MRP-80 for 10 min when testing magnetic field increased to 450 mT; (c) an 800 mT magnetic field was applied to I-MRP-80 for 10 min when testing magnetic field was increased to 450 mT; (d) an 800 mT magnetic field was applied to the isotropic sample for 10 min before testing (A-MRP-80).

and  $G'$  than those of I-MRP and the fully pre-configured MRP (A-MRP) achieves even higher values. In this work, we find that the freshly prepared MRP material can be fully pre-configured under an 800 mT magnetic field (10 min). The fully pre-configured MRP material (A-MRP) shows stable dynamic properties, as shown in Fig. S2, ESI†.

Fig. 11 depicts the dependence of the loss factor ( $\tan\delta$ ) of MRP-80 with different iron particle distribution on the magnetic flux density.  $\tan\delta$  of I-MRP-80 is larger than that of A-MRP-80 when the magnetic field is smaller than 400 mT. Above 400 mT, the two  $\tan\delta$  are almost coincident. The reason for this can be explained: at first, the iron particles in the I-MRP can freely change their locations when a magnetic field is applied. Thus the energy dissipation caused by interfacial slipping between iron particles and the matrix should be taken into account. Secondly, the magnetic interactions of I-MRP are smaller than those for A-MRP under a low magnetic field. As a result, the restriction effect in I-MRP to the soft segments in the matrix is weaker than that in A-MRP (as shown in Fig. 7a and Fig. 7c), which causes higher damping. When the magnetic field reaches over 400 mT, the restriction effect on the matrix will be coincident for the two products with different iron particle distribution. In addition, the iron particles in I-MRP will almost stop moving when the magnetic field increases to a large value and the energy dissipation for interfacial slipping can be ignored. Therefore,  $\tan\delta$  of the two MRP products with different

**Table 2** The main parameters of dynamic properties for MRP-80 with different pretreatment processes

MRP state	Initial storage modulus $G_0'$ /MPa	Magneto-induced modulus $\Delta G'/\text{MPa}$	Relative MR effect $\Delta G'/G_0'$	Minimum loss factor $\tan\delta$
A-MRP-80	1.23	6.54	532%	0.03
I-MRP-80	0.56	6.86	1225%	0.03

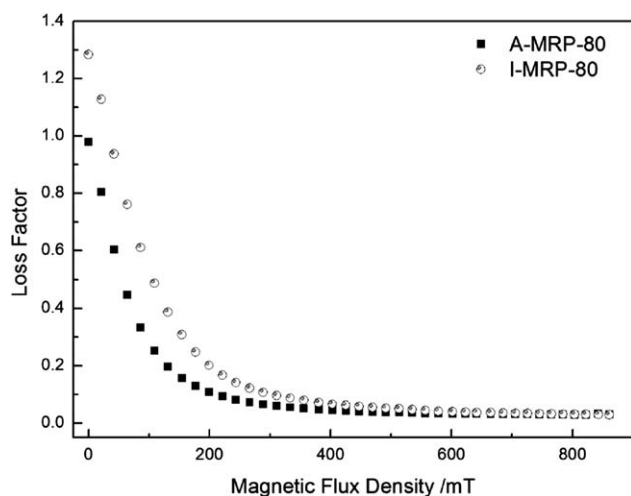


Fig. 11 Loss factors of MRP-80 with different pretreatment processes under different magnetic flux density.

iron particle distributions show similar damping properties after the magnetic field increases to 400 mT.

### 3.4 Influence of temperature on the dynamic properties

In this work, the temperature influence on the dynamic properties of the A-MRP material was studied. The A-MRP-80 was used for testing again. The relationship between the dynamic properties and magnetic flux density under different temperatures are shown in Fig. 12 and Fig. 13. It can be seen from Fig. 12 that  $G'$  decreases when increasing the temperature. However, when the temperature is higher than 40 °C, the temperature effect for the product is not so obviously, which means the MRP material is stable under high temperature. As we know, PU is a sort of temperature dependent viscoelastic material. Increasing the temperature, the PU matrix becomes softer which will lead to the decrease of  $G_0'$ .  $\Delta G'$  is mainly caused by the magnetic interactions between iron particles and the temperature has nearly no

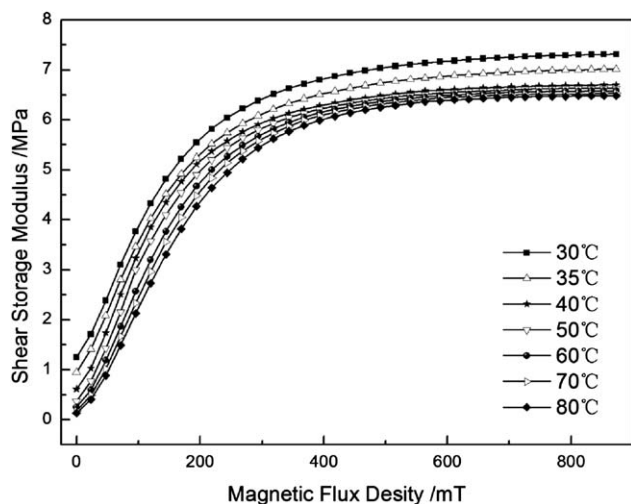


Fig. 12 Storage moduli of A-MRP-80 under different temperatures and different magnetic flux density.

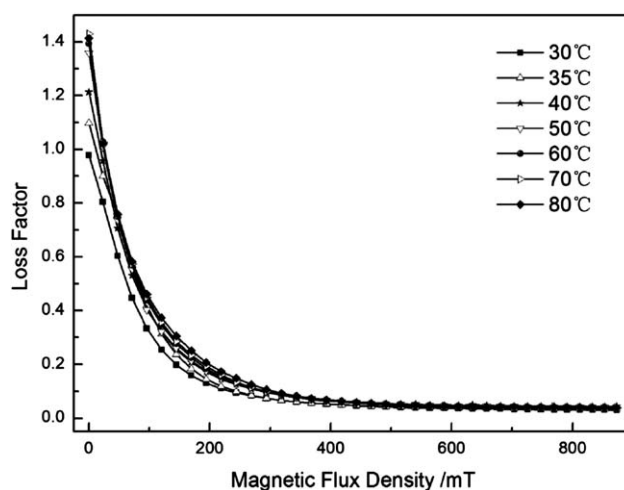


Fig. 13 Loss factors of A-MRP-80 under different temperatures and different magnetic flux density.

influence on magnetic interactions. Therefore,  $\Delta G'$  hardly changes when the temperatures is increased.

Fig. 13 shows the temperature dependency of  $\tan\delta$ . As shown in the curves,  $\tan\delta$  increases with increasing temperature under a low magnetic field. If the magnetic field exceeds 400 mT,  $\tan\delta$  tends to a similar value. In this case, when the temperature increases, the movement of the soft segments in polyurethane will become intense and then a high  $\tan\delta$  is achieved. However, with further increasing of the magnetic field, the movement of the soft segments will be restricted by magnetic interactions between iron particles. The restriction effect is the same under the same magnetic field because the iron particle content and their arrangements are identical. Therefore,  $\tan\delta$  are coincident when magnetic field exceeds 400 mT. In combination with the analysis above, it is clear that the A-MRP material is stable at a certain range of temperatures and it also shows low temperature dependency. These results may enable the MRP material be widely used in practical applications.

## 4 Conclusions

In this work, a new high-performance MR material with relatively high MR effect and low loss factor was prepared by using plastic polyurethane (PU) as the matrix. This as-prepared MR elastomer (MRP) material is similar to the plasticene and the shapes of it can be changed to various forms. The dynamic properties of MRP were systematically tested and the relationships between dynamic properties and magnetic field, iron particle content, iron particle distribution, and temperature were analyzed. The MRP material shows a higher MR performance than the previously reported MRE under similar testing conditions. For the anisotropic MRP, the maximum magneto-induced storage modulus is 6.54 MPa and the relative MR effect reaches as high as 532% and the isotropic MRP can reach even higher values (6.86 MPa and 1225%). The loss factor can be reduce to 0.03, which is much lower than that of MRE. The problems, such as particles sediment and aggregations, which may preclude some applications of MRF and MRG do not exist in the MRP material. In addition, this MRP material shows some distinctive

properties, such as self-assembling properties, high magneto-sensitivity, and a unique damping property under an external magnetic field, *etc.* Due to its unique properties and high MR performance, this kind of MRP material may widen the potential application of these MR materials.

## Acknowledgements

Financial support from NSFC (Grant No. 11072234), SRFDP of China (Project No.20093402110010), and the Fundamental Research Funds for the Central Universities are gratefully acknowledged.

## References

- 1 J. D. Carlson and M. R. Jolly, *Mechatronics*, 2000, **10**, 555.
- 2 T. Shiga, A. Okada and T. Kurauchi, *J. Appl. Polym. Sci.*, 1995, **58**, 787.
- 3 A. Fuchs, M. Xin, F. Gordaninejad, X. J. Wang, G. H. Hitchcock, H. Gecol, C. Evrensel and G. Korol, *J. Appl. Polym. Sci.*, 2004, **92**, 1176.
- 4 J. Kaleta and D. Lewandowski, *Smart Mater. Struct.*, 2007, **16**, 1948.
- 5 J. M. Ginder, L. C. Davis and L. D. Elie, *Int. J. Mod. Phys. B*, 1996, **10**, 3293.
- 6 H. M. Yin and L. Z. Sun, *Appl. Phys. Lett.*, 2005, **86**, 261901.
- 7 M. Zubieta, S. Eceolaza, M. J. Elejabarrieta and M. M. Bou-Ali, *Smart Mater. Struct.*, 2009, **18**, 095019.
- 8 C. Xiong, J. G. Lu, J. Q. Zhang, and Z. N. Li, *Proceedings of the 4th International Conference on Nonlinear Mechanics*, 2002, 845.
- 9 W. H. Li and H. Du, *Int. J. Adv. Manuf. Technol.*, 2003, **21**, 508.
- 10 H. J. Jung, B. F. Spencer and I. W. Lee, *J. Struct. Eng.*, 2003, **129**, 873.
- 11 M. Brigley, Y. T. Choi, N. M. Wereley and S. B. Choi, *J. Intell. Mater. Syst. Struct.*, 2007, **18**, 1143.
- 12 M. J. Wilson, A. Fuchs and F. Gordaninejad, *J. Appl. Polym. Sci.*, 2002, **84**, 2733.
- 13 B. Hu, A. Fuchs, S. Huseyin, F. Gordaninejad and C. Evrensel, *J. Appl. Polym. Sci.*, 2006, **100**, 2464.
- 14 X. L. Gong, X. Z. Zhang and P. Q. Zhang, *Polym. Test.*, 2005, **24**, 669.
- 15 A. Boczkowska, S. F. Awietjan and R. Wroblewski, *Smart Mater. Struct.*, 2007, **16**, 1924.
- 16 B. K. S. Woods, N. Wereley, R. Hoffmaster and N. Nersessian, *Int. J. Mod. Phys. B*, 2007, **21**, 5010.
- 17 J. M. Ginder, W. F. Schlotter and M. E. Nichols, *Smart Structures and Materials 2001: Damping and Isolation*, 2001, **4331**, 103.
- 18 A. M. Albanese and K. A. Cunefare, *Smart Structures and Materials 2003: Damping and Isolation*, 2003, **5052**, 36.
- 19 H. X. Deng, X. L. Gong and L. H. Wang, *Smart Mater. Struct.*, 2006, **15**, N111.
- 20 H. L. Sun, P. Q. Zhang, X. L. Gong and H. B. Chen, *Journal of Sound and Vibration*, 2007, **300**, 117.
- 21 N. Hoang, N. Zhang and H. Du, *Smart Mater. Struct.*, 2009, **18**, 074009.
- 22 C. Bellan and G. Bossis, *Int. J. Mod. Phys. B*, 2002, **16**, 2447.
- 23 S. A. Demchuk and V. A. Kuz'min, *Journal of Engineering Physics and Thermophysics*, 2002, **75**, 396.
- 24 L. Chen, X. L. Gong, W. Q. Jiang, J. J. Yao, H. X. Deng and W. H. Li, *J. Mater. Sci.*, 2007, **42**, 5483.
- 25 X. L. Gong, L. Chen and J. F. Li, *Int. J. Mod. Phys. B*, 2007, **21**, 4875.
- 26 A. V. Chertovich, G. V. Stepanov, E. Y. Kramarenko and A. R. Khokhlov, *Macromol. Mater. Eng.*, 2010, **295**, 336.
- 27 B. Wei, X. L. Gong and W. Q. Jiang, *J. Appl. Polym. Sci.*, 2010, **116**, 771.
- 28 A. Fuchs, Q. Zhang, J. Elkins, F. Gordaninejad and C. Evrensel, *J. Appl. Polym. Sci.*, 2007, **105**, 2497.
- 29 M. Furukawa, Y. Mitsui, T. Fukumaru and K. Kojio, *Polymer*, 2005, **46**, 10817.
- 30 A. Boczkowska and S. F. Awietjan, *J. Mater. Sci.*, 2009, **44**, 4104.
- 31 D. Z. Ma, M. Z. Wang, M. C. Zhao, X. Y. Zhang and X. L. Luo, *J. Polym. Sci., Part B: Polym. Phys.*, 1999, **37**, 2918.
- 32 L. C. Davis, *J. Appl. Phys.*, 1999, **85**, 3348.
- 33 T. H. Boyer, *Am. J. Phys.*, 1988, **56**, 688.
- 34 H. Bose and R. Roder, *J. Phys.: Conference Series*, 2009, **149**, 1.
- 35 L. Chen, X. L. Gong and W. H. Li, *Smart Mater. Struct.*, 2007, **16**, 2645.
- 36 R. Chandra, S. P. Singh and K. Gupta, *Compos. Struct.*, 1999, **46**, 41.
- 37 L. Chen, X. L. Gong and W. H. Li, *Chinese J. Chem. Phys.*, 2008, **21**, 581.